

Probing the nature of dark matter with Cosmic X-rays: Constraints from “Dark blobs” and grating spectra of galaxy clusters

Signe Riemer-Sorensen¹, Kristian Pedersen¹, Steen H. Hansen¹, and Haakon Dahle²

¹ *Dark Cosmology Centre, Niels Bohr Institute, University of Copenhagen,*

Juliane Maries Vej 30, DK-2100 Copenhagen, Denmark

² *Institute of Theoretical Astrophysics, University of Oslo,*

P.O. Box 1029, Blindern, N-0315 Oslo, Norway

(Dated: November 23, 2017)

Gravitational lensing observations of galaxy clusters have identified dark matter “blobs” with remarkably low baryonic content. We use such a system to probe the particle nature of dark matter with X-ray observations. We also study high resolution X-ray grating spectra of a cluster of galaxies. From these grating spectra we improve the conservative constraints on a particular dark matter candidate, the sterile neutrino, by more than one order of magnitude. Based on these conservative constraints obtained from Cosmic X-ray observations alone, the low mass ($m_s \lesssim 10$ keV) and low mixing angle ($\sin^2(2\theta) \lesssim 10^{-6}$) sterile neutrino is still a viable dark matter candidate.

PACS numbers:

I. INTRODUCTION

The cosmological dark matter abundance is firmly established through observations of the cosmic microwave background and of the large scale structure of the universe [1, 2]. This is complemented by measurements of dark matter on smaller scales by studies of, e.g. the rotation curves of galaxies, gravitational lensing by galaxies and clusters of galaxies [3], the velocity dispersion of galaxies in clusters of galaxies, and X-ray emitting hot gas in clusters of galaxies [4]. However, the particle nature of dark matter remains a puzzle.

There are numerous dark matter candidates, among which the sterile neutrino is particularly well motivated. The sterile neutrino is a natural dark matter candidate in a minimally extended standard model of particle physics [11] and it provides solutions to other problems: the masses of the active neutrinos [7], the baryon asymmetry of the Universe [8], and the observed peculiar velocities of pulsars [9, 10]. Sterile neutrinos participate in the flavour-mass eigenstate oscillations of the active standard model neutrinos, and are thereby allowed to decay radiatively through a two-body decay with photon energy predicted to lie in the X-ray range ($E_\gamma = m_s/2$, where m_s is the rest mass of the sterile neutrino). This renders it a testable dark matter candidate [12].

The decay rate of any dark matter candidate with a radiative two-body decay can be constrained from observations of dark matter concentrations (for references see [13, 14, 15]). The strongest constraints are obtained from studying dark matter dominated regions, and with instruments with high spectral resolution (since the decay line is expected only to suffer negligible broadening).

Recent gravitational lensing observations of the mass distribution in galaxy clusters [5] have identified cluster scale dark matter “blobs” with very low baryonic content. This allows for the novel possibility of using such almost pure dark matter blobs to probe the particle nature of the dark matter [6]. Below we analyze X-ray observations of

the dark matter blob in the cluster of galaxies Abell 520. Also, we analyze high resolution X-ray grating spectra of the cluster of galaxies Abell 1835, allowing us to improve constraints from earlier studies by more than one order of magnitude.

II. X-RAY DATA ANALYSIS

When a spectrum has been obtained from an observation of a given dark matter dense region, there are different ways of searching for a hypothetical mono-energetic emission line and to determine an upper limit on the flux from decaying dark matter particles. The simplest and most conservative method is the “slice method,” where the energy range of the spectrum is divided into bins of a width equal to the instrumental energy resolution (2σ), and all of the X-ray flux in a particular bin is determined from a model fitted to the spectrum. The slice method is very robust, as the physics behind the fitted model is irrelevant, and the method does not require any assumptions about the X-ray background, but regards all received flux as an upper limit for the flux from decaying dark matter. This is despite the fact that the total flux is known to consist of several contributions; the cosmic X-ray background from unresolved sources, the X-ray emission from the intra cluster medium, the Milky Way halo, and the instrumental background. The “slice method” takes into account that an emission line from decaying dark matter could “hide” under a line feature in the spectrum [16]. Other methods for constraining the flux (for example [17]) can give stronger, but less robust, results (for a discussion of different methods see [18]). In this study, we conservatively use the slice method.

III. GRATING OBSERVATIONS OF THE GALAXY CLUSTER ABELL 1835

A good spectral resolution is required to search for a mono-energetic emission line. The high spatial resolution of the *Chandra* X-ray telescope can be turned into a very high spectral resolution (≈ 5 eV) by deflecting the incoming photons in a grating, as the deflection angle is highly sensitive to the photon energy. The ACIS-HETG instrument consists of two gratings, which on demand can be placed between the mirrors and the ACIS CCDs: the High Energy Grating (0.8–9.0 keV), HEG, and the Medium Energy Grating, MEG (0.4–5.0 keV) [33].

When the incoming photons are deflected in a grating, the information of their spatial origin is lost. This makes it impossible to optimize the ratio of expected dark matter signal to noise from X-ray emitting baryons in the observational field of view (as described by [15, 16]). In this study, the cluster of galaxies Abell 1835 was targeted because most of the emission from the cluster comes from a region close to the observational axis making grating spectroscopy possible. Abell 1835 has a luminosity distance of $D_L = 1225$ Mpc ($z = 0.252$, [19]), and the mass within the scale radius of $R \approx 800$ kpc ≈ 4.2 arcmin is $M_{fov}^{A1835} = 6.5 \times 10^{14} M_\odot$ [20]. No other obvious mass concentrations are seen in the field of view. (Here, and in the following, a cosmology with $\Omega_m = 0.26$, $\Omega_\Lambda = 0.74$, $h = 0.71$ is assumed).

The spectral resolution of a grating spectrometer decreases proportionally to the angular extension of the source. For Abell 1835 the emission is dominated by photons from within the core radius, $r_c = 39 \pm 3$ kpc ≈ 10 arcsec [19] so this characteristic radius was used to determine the spectral resolution [34]:

$$\begin{aligned} \sigma_{HEG} &\approx \frac{(E_\gamma / \text{keV})^2}{156m} \text{ keV} \\ \sigma_{MEG} &\approx \frac{(E_\gamma / \text{keV})^2}{78m} \text{ keV}, \end{aligned} \quad (1)$$

where m is the dispersion order. Grating spectra of Abell 1835 were extracted from the observation with id 511 using CIAO 3.3 [35]. The first order deflections were combined into a single spectrum with a spectral bin size of 0.006 keV and 0.013 keV (at $E_\gamma = 1$ keV) for HEG and MEG, respectively. The line broadening due to the velocity dispersion of dark matter in Abell 1835 is negligible ($v/c \approx 10^{-5} - 10^{-4}$).

With the spectral fitting package Sherpa [21], a thermal plasma model (MEKAL, [22]) was fitted to the data with the temperature and abundance as free parameters. The model is an adequate representation of the data, giving a reduced χ^2 of 1.2 in both cases (683 and 569 degrees of freedom for HEG and MEG, respectively). The flux was determined using the slice method for a slice width given by eq. 1.

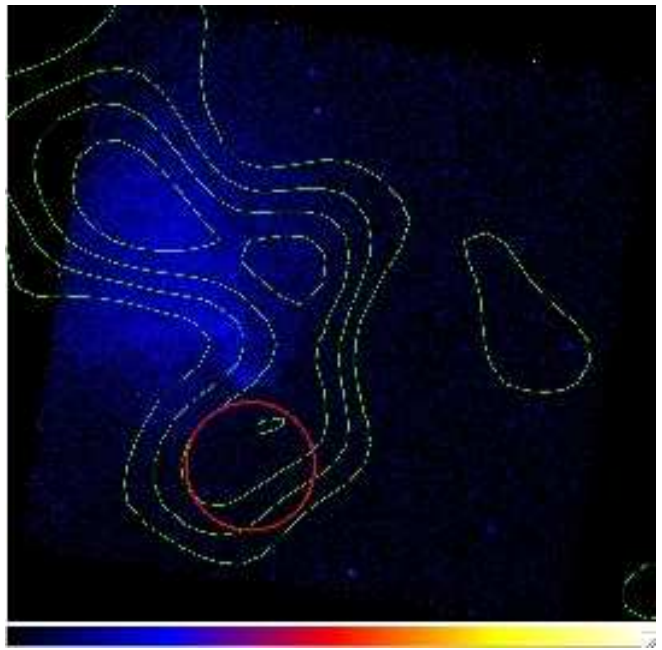


FIG. 1: (Color online) Abell 520 observed in X-rays (0.3–10.0 keV, blue color) with *Chandra* with the gravitational potential from weak lensing overlaid (green contours). The dark matter blob in the red circle has very low X-ray emission from baryons.

IV. THE DARK MATTER BLOB IN THE GALAXY CLUSTER ABELL 520

For direct imaging data the field of view can be optimized by observing a dark matter dense region with low X-ray emission from baryons. A unique example is the merging cluster of galaxies Abell 520 containing a “blob” of high mass concentration with very low X-ray emission discovered recently using weak gravitational lensing [23], see FIG. 1 [36].

An ACIS-S3 0.3–9.0 keV spectrum was extracted from the *Chandra* observation with id 4215 for a region centred at the dark blob ($RA, DEC = 04^{\text{h}}54^{\text{min}}04.036^{\text{s}}, +02^{\circ}52'37.30''$) and with a radius of $r = 0.85$ arcmin = 190 kpc (the red circle in FIG. 1). A model consisting of a power law and six Gaussians was fitted to the spectrum with a reduced χ^2 of 1.2 (for 80 degrees of freedom). The flux was determined using the slice method for a slice width given by the resolution of ACIS-S3 [37]:

$$\sigma_{S3} = 0.005E_\gamma + 0.05 \text{ keV} \quad (2)$$

The mass of the dark matter blob in A520 has been derived from weak gravitational lensing to be $M_{fov}^{blob} = 4.78 \pm 1.5 \times 10^{13} h^{-1} M_\odot$. This value is based on measuring the overdensity in the blob region with respect to the mean density in a surrounding annulus with inner and outer radius of 0.85 arcmin and 4 arcmin, respectively. Hence, the mass value can be regarded as a conservative

lower limit on the mass contained within the blob region. A detailed description of the data and methodology of the weak lensing analysis is given elsewhere [24].

The luminosity distance to A520 is $D_L = 980$ Mpc ($z = 0.203$, [25]).

V. DECAY RATE

Let us now consider a specific dark matter candidate, the sterile neutrinos. They can decay radiatively as $\nu_s \rightarrow \nu_\alpha + \gamma$, where ν_α is an active neutrino. This is a two-body decay with a photon energy of $E_\gamma = m_s/2$. Assuming only one kind of dark matter, the observed flux, F_{obs} , at a given photon energy yields an upper limit on the flux from two-body radiatively decaying dark matter:

$$\Gamma_\gamma \leq \frac{8\pi F D_L^2}{M_{fov}}. \quad (3)$$

The Milky Way dark matter halo will always be included in the observation, and its mass contribution to the total mass in the field of view has to be taken into account [13, 16]. For the Milky Way we use a virial mass of $M_{halo}^{vir} = 10^{12} M_\odot$ and by integration of a NFW profile we find the halo mass to have a mean distance of 35 kpc. The halo mass and mean distance varies less than a factor of two for a reasonable range of model parameters [16]. For the grating observation of Abell 1835 the Milky Way halo mass within the field of view is $M_{halo}^{A1835} = 9 \times 10^5 M_\odot$, and for the dark matter blob in Abell 520 it is $M_{halo}^{A520} = 4 \times 10^3 M_\odot$.

FIG. 2 shows the upper limit on the decay rate of any dark matter candidate (given by eq. 3) obtained from the total amount of received flux for the Abell 520 dark matter blob and the Abell 1835 grating data. It is seen that the grating data of Abell 1835 provide constraints that are one to two orders of magnitude stronger than the constraints obtained from observations of the Milky Way halo alone [16, 17]. Also, the data from the blob of Abell 520 provide stronger constraints than the Milky Way halo.

The constraints on the decay rate from the grating data of Abell 1835 can be approximated by an analytical expression for HEG and MEG independently. As seen in FIG. 3, a second order polynomial describes the HEG constraints quite well, and a sixth order polynomial fits the MEG data:

$$\begin{aligned} \Gamma_{HEG} &= -8.6 \cdot 10^{-28} + 1.7 \cdot 10^{-27} E_\gamma - 1.5 \cdot 10^{-28} E_\gamma^2 \\ \Gamma_{MEG} &= -2.9 \cdot 10^{-28} + 1.4 \cdot 10^{-27} E_\gamma + 9.7 \cdot 10^{-28} E_\gamma^2 \\ &\quad - 5.4 \cdot 10^{-28} E_\gamma^3 + 1.1 \cdot 10^{-28} E_\gamma^4 \\ &\quad - 1.3 \cdot 10^{-29} E_\gamma^5 + 6.4 \cdot 10^{-31} E_\gamma^6. \end{aligned} \quad (4)$$

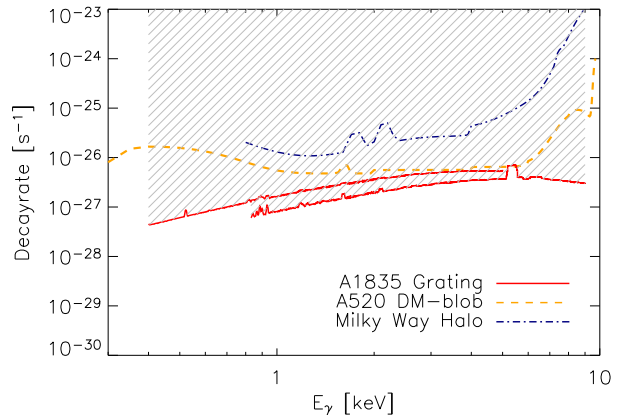


FIG. 2: (Color online) The upper limit on the radiative two-body decay rate obtained from the dark matter blob of Abell 520 (dashed) and the grating spectra of Abell 1835 (solid) shown together with the Milky Way halo constraint [16] (dot-dashed).

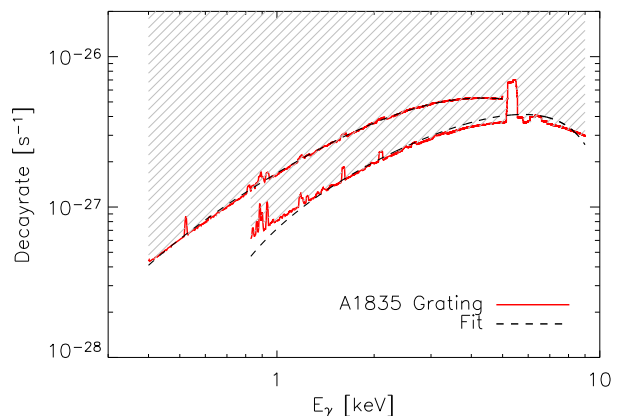


FIG. 3: (Color online) The Abell 1835 grating spectrum upper limit on the decay rate and its approximate analytical expression given by of eq. 4.

VI. CONSTRAINING MASS AND MIXING ANGLE

By regarding all decay branches possible through oscillations, the mean lifetime of a sterile Dirac neutrino of mass, m_s , has been determined to be [26, 27]:

$$\tau = \frac{1}{\Gamma_{tot}} = \frac{f(m_s) \cdot 10^{20}}{(m_s/\text{keV})^5 \sin^2(2\theta)} \text{sec}^{-1}, \quad (5)$$

where Γ_{tot} is the total decay rate. $f(m_s)$ takes into account the open decay channels so that for $m_s < 1$ MeV, where only the neutrino channel is open, $f(m_s) = 0.86$. For Majorana neutrinos, which we will be considering below, $f(m_s)$ is half the value for Dirac neutrinos. The branching ratio of the radiative decay is $\Gamma_\gamma/\Gamma_{tot} =$

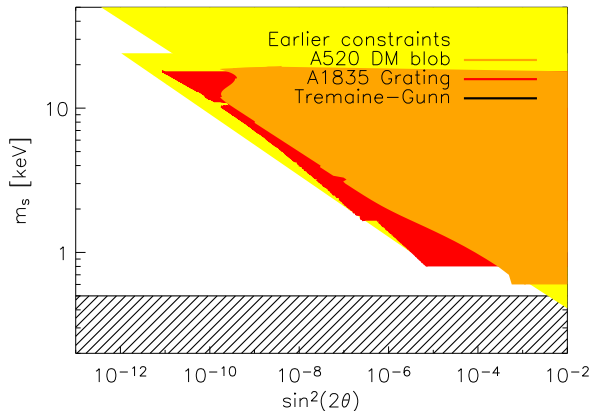


FIG. 4: (Color online) The observational constraints from the grating spectrum of Abell 1835 (red) and the dark matter blob of A520 (orange) together with the Tremaine-Gunn limit (black, [28]) and earlier X-ray constraints (yellow, [13, 15, 16, 17, 29]).

$27\alpha/8\pi \approx 1/128$ [26]. This can be combined with eq. 3 to give:

$$\sin^2(2\theta) \lesssim 7 \times 10^{17} \text{sec}^{-1} \left(\frac{F_{det}}{\text{erg/cm}^2/\text{sec}} \right) \left(\frac{m_s}{\text{keV}} \right)^{-5} (6) \\ \times \left[\frac{(M_{fov}/M_\odot)}{(D_L/\text{Mpc})^2} + \frac{(M_{halo}/M_\odot)}{(D_{halo}/\text{Mpc})^2} \right]^{-1}.$$

The observational constraints in the $\sin^2(2\theta) - m_s$ parameter space are shown in FIG. 4 for the grating spectrum of Abell 1835 (red) and the dark matter blob of A520 (orange) together with the Tremaine-Gunn limit (black, [28]) and earlier X-ray constraints (yellow, [13, 15, 16, 17, 29]). It is seen that even though no optimization of the field of view can be performed for the grating data, the improvement of instrumental spectral resolution leads to superior constraints. The grating constraints are very robust as they have been derived from the total amount of received X-ray flux without subtrac-

tion of any background contributions. The earlier constraints are derived by less robust and more model dependent methods.

VII. CONCLUSIONS

A very general constraint on the decay rate for all dark matter particle candidates with a two-body radiative decay in the X-ray range has been derived. We have analyzed grating spectra of the galaxy cluster Abell 1835, and a spectrum obtained through direct imaging of the almost pure dark matter blob in the galaxy cluster Abell 520. These provide the strongest constraints on radiatively decaying dark matter derived in a very conservative way from cosmic X-ray data. The mass and mixing angle can be constrained in the specific case of sterile neutrinos, leaving a low mass ($m_s \lesssim 10$ keV) and low mixing angle ($\sin^2(2\theta) \lesssim 10^{-6}$) window open. However, combined with other methods [30, 31], the Dodelson-Widrow scenario for sterile neutrino production could soon be ruled out. Other mechanisms for production of sterile neutrinos, for example, via inflaton decays [32], would satisfy all the constraints.

The obtained constraints can be improved significantly by improving the signal to noise ratio (optimization of field of view) and by improving the instrumental spectral resolution. This could be realized through X-ray grating observations of dark matter dense regions or the Milky Way halo (blank sky fields).

Acknowledgments

The Dark Cosmology Centre is funded by the Danish National Research Foundation. KP acknowledges support from Instrument Center for Danish Astrophysics. We thank M. Shaposhnikov for pleasant and useful discussions, and A. Boyarsky and O. Ruchayskiy for useful comments.

-
- [1] D. N. Spergel *et al.* [WMAP Collaboration], *Astrophys. J. Suppl.* **148**, 175 (2003)
 - [2] U. Seljak *et al.* [SDSS Collaboration], *Phys. Rev. D* **71**, 103515 (2005)
 - [3] P. Schneider, in proceedings of the XIV Canary Islands Winter School of Astrophysics, arXiv:astro-ph/0306465
 - [4] P. Rosati, S. Borgani and C. Norman, *Ann. Rev. Astron. Astrophys.* **40**, 539 (2002)
 - [5] D. Clowe, M. Bradac, A. H. Gonzalez, M. Markevitch, S. W. Randall, C. Jones and D. Zaritsky, arXiv:astro-ph/0608407.
 - [6] S. H. Hansen, J. Lesgourgues, S. Pastor and J. Silk, *Mon. Not. Roy. Astron. Soc.* **333**, 544 (2002)
 - [7] T. Asaka, S. Blanchet and M. Shaposhnikov, *Phys. Lett. B* **631**, 151 (2005)
 - [8] T. Asaka and M. Shaposhnikov, *Phys. Lett. B* **620**, 17 (2005)
 - [9] G. M. Fuller, A. Kusenko, I. Mocioiu and S. Pascoli, *Phys. Rev. D* **68**, 103002 (2003)
 - [10] A. Kusenko and G. Segre, *Phys. Lett. B* **396**, 197 (1997)
 - [11] S. Dodelson and L. M. Widrow, *Phys. Rev. Lett.* **72**, 17 (1994)
 - [12] A. D. Dolgov and S. H. Hansen, *Astropart. Phys.* **16**, 339 (2002)
 - [13] A. Boyarsky, A. Neronov, O. Ruchayskiy, M. Shaposhnikov and I. Tkachev, arXiv:astro-ph/0603660.

- [14] K. Abazajian and S. M. Koushiappas, *Phys. Rev. D* **74** (2006) 023527
- [15] C. R. Watson, J. F. Beacom, H. Yuksel and T. P. Walker, *Phys. Rev. D* **74**, 033009 (2006)
- [16] S. Riemer-Sorensen, S. H. Hansen and K. Pedersen, *Astrophys. J.* **644**, L33 (2006)
- [17] A. Boyarsky, A. Neronov, A. Neronov, O. Ruchayskiy and M. Shaposhnikov, arXiv:astro-ph/0603368.
- [18] Signe Riemer-Sorensen, Masters Thesis, “Sterile neutrinos as a dark matter candidate”, <http://www.dark-cosmology.dk>
- [19] R. W. Schmidt, S. W. Allen and A. C. Fabian, *Mon. Not. Roy. Astron. Soc.* **327**, 1057 (2001)
- [20] L. M. Voigt and A. C. Fabian, *Mon. Not. Roy. Astron. Soc.* **368**, 518 (2006)
- [21] P. E. Freeman, S. Doe and A. Siemiginowska, SPIE Proceedings, Vol. 4477, p.76, 2001 arXiv:astro-ph/0108426.
- [22] R. Mewe, E. H. B. M. Gronenschild, and G. H. J. van der Oord, 1985, *A&As*, 62, 197.
- [23] M. Markevitch, F. Govoni, G. Brunetti, and D. Jerius, *Astrophys. J.* **627**, 733 (2005)
- [24] H. Dahle, N. Kaiser, R. J. Irgens, P. B. Lilje, and S. J. Maddox, *Astrophysical Journal Supplement Series*, 139:313-368 (2002)
- [25] H. Ebeling, *et al.*, *MNRAS*, 301, 881 (1998)
- [26] V. D. Barger, R. J. N. Phillips and S. Sarkar, *Phys. Lett. B* **352**, 365 (1995) [Erratum-ibid. B **356**, 617 (1995)]
- [27] A. D. Dolgov, S. H. Hansen, G. Raffelt and D. V. Semikoz, *Nucl. Phys. B* **590**, 562 (2000)
- [28] S. Tremaine and J. E. Gunn, *Phys. Rev. Lett.* **42**, 407 (1979)
- [29] A. Boyarsky, A. Neronov, O. Ruchayskiy and M. Shaposhnikov, *Mon. Not. Roy. Astron. Soc.* **370**, 213 (2006)
- [30] U. Seljak, A. Makarov, P. McDonald and H. Trac, arXiv:astro-ph/0602430.
- [31] M. Viel, J. Lesgourgues, M. G. Haehnelt, S. Matarrese and A. Riotto, *Phys. Rev. D* **71**, 063534 (2005)
- [32] M. Shaposhnikov and I. Tkachev, *Phys. Lett. B* **639**, 414 (2006)
- [33] <http://cxc.harvard.edu/proposer/POG/html>, http://space.mit.edu/CSR/hetg_info.html
- [34] <http://cxc.harvard.edu/proposer/POG/html>
- [35] <http://cxc.harvard.edu/ciao>
- [36] A similar analysis of the dark matter concentration in the bullet cluster has been carried out by Boyarsky et al. Their findings are qualitatively similar to the blob results presented here (private communication with M. Shaposhnikov)
- [37] <http://cxc.harvard.edu/proposer/POG/html>